Tuning Mechanical Behavior of Polymer Materials via Multi-Arm Crosslinked Network Architectures

Peter J. Hayes
Department of Mechanical and Manufacturing Engineering, Miami University, Oxford, OH, 45056, USA

Dominik Konkolewicz
Department of Chemistry and Biochemistry, Miami University, Oxford, OH 45056, USA

Mehdi B. Zanjani*
Department of Mechanical and Manufacturing Engineering, Miami University, Oxford, OH 45056, USA

Crosslinked polymer materials provide tremendous opportunities for delivering unique material properties for a wide variety of applications such as shape-memory and self-healing materials, aerospace materials, and biomedical systems. Most crosslinked polymer networks investigated to date are designed based on covalent or noncovalent crosslinkers that include two-ended connections to the backbone polymer base. In this paper, we investigate the topic of multi-arm crosslinking of polymer materials using a computational platform. We take advantage of Molecular Dynamics (MD) simulations and graph theory to define computational models that describe potential architectures for multi-arm crosslinked polymer networks. We also discuss feasible experimental routes for implementation of these approaches. We investigate how the polymer network architecture affects the mechanical and self-healing behavior of the material. Our results show that the angular stiffness of multi-arm crosslinkers can be adjusted to control the mechanical strength of the overall polymer network. Additionally, using graph theory, we find that the complex connections that exist between the crosslinkers and the backbone polymer chains define the overall connectivity of the polymer network, which in turn dictates the mechanical behavior of the material. Furthermore, we find that increasing the number of crosslinking arms may improve the self-healing behavior, but it can reduce the overall mechanical strength of the polymer network. The findings of this work can motivate future experimental and data-driven studies to realize more sophisticated crosslinked polymer materials with a large number of degrees of freedom to deliver a variety of tunable properties.

I. INTRODUCTION

Crosslinked polymers have been the focus of many recent studies as they provide a variety of enhanced material properties for applications such as shape-memory materials, biomedical systems, and optical communication devices [1–4]. Dynamic crosslinking in polymer networks has been shown to provide enhanced self-healing and mechanical properties [5–9]. Both covalent and noncovalent crosslinkers have been utilized to build dynamic crosslinked polymer networks that provide strong and stimulus-responsive materials with desirable self-healing and malleability properties [10–21]. It has been shown that the structure of crosslinked polymer materials and the overall architecture of polymer networks can be used to tune various material properties such as the mechanical and self-healing behaviors [17–19, 22–24]. The crosslinking mechanism in such materials is mainly based on two crosslinking arms per crosslinker, each connecting to a potential binding site on the backbone polymer chains [17–22]. Consequently, for a vast majority of the crosslinked polymer materials studied to date, tuning the architecture of the polymer network mainly involves adjusting crosslinking percentage and the basic properties of the backbone polymer chains [22, 23]. In order to increase the number of degrees of freedom to control the architecture and properties of polymer networks, utilizing more complex crosslinking agents can provide new promising opportunities. For example, carbon nanotubes or nanoparticles of different types have been utilized to improve mechanical, thermal, and electrical properties of polymer materials [25–28]. In such systems the crosslinking mechanism facilitates strong connections between backbone polymer chains and the reinforcing cores of nanoparticles or nanotubes. A natural way to imagine more complex designs for crosslinkers is to increase the number of crosslinking arms per crosslinking agent, and therefore considering crosslinking agents with more than two arms to connect to backbone polymer chains within a network. We use the terminology 'multi-arm crosslinkers' to refer to such crosslinking agents, which by nature, introduce a large parameter space to be explored within the design of polymer networks. The structure and properties of polymer networks with multi-arm crosslinkers is largely unexplored in the relevant scientific literature. Computational techniques can provide a promising tool for this purpose [22, 24, 29–37] in order to investigate how adjusting a wide range of parameters can change the overall architecture of multi-arm polymer networks and the resulting material properties.

This article sets out to investigate the structure and properties of multi-arm crosslinked polymer networks utilizing a computational platform based on molecular simu-

* zanjanm@miamioh.edu

lations and graph theory. We consider two different categories of multi-arm crosslinkers and build coarse grained molecular dynamics models of the corresponding overall polymer networks. We then investigate how the architecture of multi-arm crosslinked networks affects the mechanical and self-healing properties of the material. Specifically, we investigate the effect of angular stiffness of crosslinkers and overall connectivity of the network on the mechanical strength of the polymer material. We then establish a graph network representation of the architecture of crosslinked material and explore the correlation between the characteristics of the graphs and the properties of the material. We also investigate the self-healing behavior of various multi-arm networks as a function of the number of crosslinking arms that define each system. Finally, we explore multi-arm polymer configurations made up of crosslinking cores of different shapes that facilitate reinforcement of the polymer material and evaluate the shape-dependent mechanical performance of such network architectures.

II. METHODOLOGY AND FRAMEWORK

We utilized coarse-grained molecular dynamics simulations to investigate polymer networks made up of multi-arm crosslinking agents. We begin by describing the overall configuration of the crosslinked polymer networks proposed in this work. Figure 1 (a), describes a sketch of crosslinked polymer networks which consist of the base background polymer chains, also known as the backbone polymer, and crosslinking agents that may become connected to the backbone chains [17, 22]. Simple crosslinkers provide a linear agent that can only connect two polymer chains, one on each crosslinking end. Multi-arm crosslinkers include more than two ends to connect various backbone chains, thus providing a larger number of degrees of freedoms that can affect both the structural architecture and the properties of the polymer network. Figure 1 (b), demonstrates the essential components of a coarse-grained model of a typical crosslinked polymer network. The background polymer chains are made up of a number of beads (n), with each bead representing a single monomer, as also described in previous literature [22, 38–40]. Each backbone polymer chain includes a number of crosslinking sites according to the specific crosslinking density considered for the system. For example, if $n = 100$ beads exist in a single polymer chain, for a crosslinking density of 7%, the system will include 7 crosslinking sites dispersed randomly within each chain, shown via the cyan color in Fig. 1 (b). The crosslinkers are also modeled using a coarse-grained framework. A simple crosslinker can be considered as a linear unit with two end beads that can bond to the crosslinking sites on the polymer backbone. Following this logic, multi-arm crosslinkers are modeled in two main categories: (1) multi-arm agents with multiple arms emerging from a center bead, and (2) a crosslinking core, with a specific shape such as cubic or spherical, covered with crosslinking agents that can connect to the polymer backbone. For the first category, we model each arm as a set of beads that are bonded together, with the outside bead, shown by purple color in Fig. 1 (b), providing the connection point to the backbone polymer chains. The arms of the crosslinker are connected to each other through a central bead, shown by the middle yellow bead. We focus on crosslinkers with three, four, five, or six arms per crosslinker in different systems throughout this study. One important feature of this crosslinking pattern is the angular stiffness corresponding to the angle between different arms of the multi-arm crosslinkers, which can provide a new important parameter to control structural features and properties of the overall polymer network. For the second category, a core that is coated with crosslinking agents acts as the multi-arm crosslinker. Therefore, each crosslinker of this type includes a core, shown by yellow beads in Fig. 1 (b), covered with crosslinking beads shown by the grey and purple beads in Fig. 1 (b). Similar to the previous case, the purple beads at the end of the arm provide the connection to the crosslinking sites on the polymer backbone. We consider various crosslinking systems of this type with different core shapes, such as spherical, cubic, and tetrahedral.

The coarse-grained MD simulations are performed within the LAMMPS [41] software package by considering each polymer chain of the backbone to be composed of $n = 100$ beads. Before analyzing the mechanical or self-healing behavior of the material, we prepare an initial configuration representing all the beads in each specific system being studied. For this purpose, each polymer chain is built as a linear chain of n beads with the corresponding number of crosslinking sites included according to a 7% value of crosslinking density. Multiple polymer chains are then reproduced and placed far enough from each other in a simulation box so that there are no overlaps between the chains initially. Similarly, we prepare multiple replicas of each crosslinker and place them far away from each other. This simulation box is then compressed during a number of NPT Molecular Dynamics simulations to reach a desired box volume that is consistent with the polymer density for an average volume fraction of around 35% or a number density of around $0.6\sigma^{-3}$ (LJ units) for different systems. For example, the model system shown in Fig. 1 (c) consists of 200 polymer chains and 400 3-arm crosslinkers, for a total of $24,000$ particles within the simulation box. During this process, the crosslinkers' end points that come in contact with the bonding sites on backbone chains will later be designated as bonded beads that interact through bonded interactions in the final MD simulations. Such crosslinking bonds are defined after the compression stage, via a postprocessing step: a crosslinking bond is defined if the center-to-center distance between a particle pair less than a cutoff distance of 1.2 times the average diameter of the two particles. Additionally, this step is followed by the whole polymer structure being

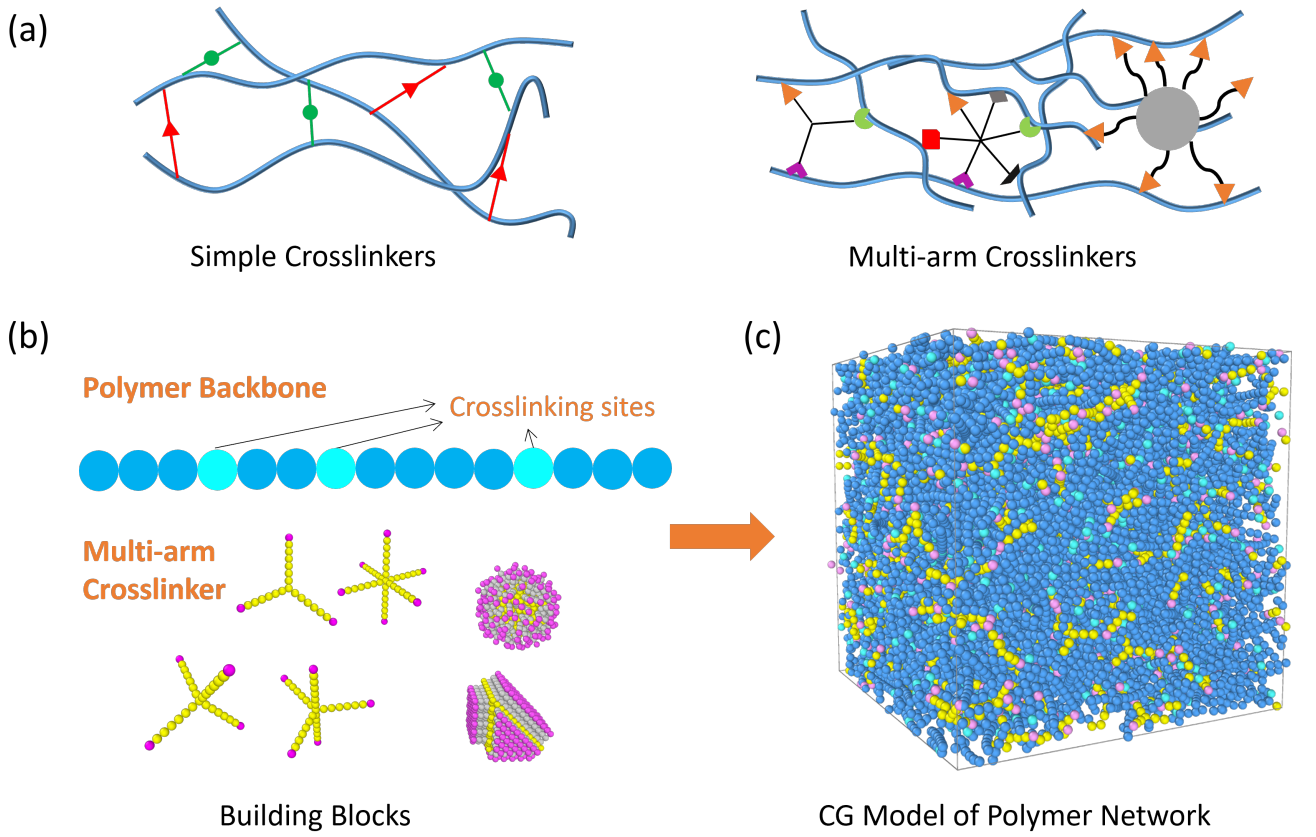

FIG. 1. (a) Schematic demonstration of polymer networks with simple and multi-arm crosslinkers. (b) The building blocks of multi-arm polymer networks, composed of the backbone polymer chains and multi-arm crosslinkers. The crosslinkers are considered to be either composed of a number arms, such as the 3-, 4-,5-, and 6-arm crosslinkers shown here, or consist of a core covered by crosslinking chains, such as the spherical and tetrahedral cores shown here. (c) Example coarse grained (CG) model of polymer network initial configuration with 3-arm crosslinkers prepared using Molecular Dynamics Simulations. Color coding is consistent with part (b).

equilibrated one more time, so that the final equilibrium structure is free from any drastic changes in particle positions or energies before the stress-strain curves are obtained. The interparticle nonbonded interactions between coarse-grained particles were modeled using the Lennard-Jones potential, $u(r) = 4\epsilon[(\sigma/r)^{12} - (\sigma/r)^{6}]$. σ represents bead diameters. ϵ represents the strength of interparticle interactions, which was set to a value of $1k_B$ T for nonbonded interactions. Covalent bonds in the system were modeled as bonded interactions in LAMMPS based on the harmonic bond potential with a strength of $K = 25\epsilon/\sigma^2$and an equilibrium distance of $r_0 = \sigma$. The angle interactions within each polymer chain and crosslinker are modeled using a harmonic angle potential following $U(\theta) = 1/2K_\theta(\theta - \theta_0)^2$, where θ_0 is the equilibrium angle and K_θ in the prefactor representing the stiffness of the angle. All the MD simulations were performed in a dimensionless format with reduced values normalized with respect to Lennard-Jones parameters. Following the initial MD simulations, the resulting equilibrium configurations are used in later MD simulations to characterize the properties of the polymer network as described in the following section.

In order to investigate the self-healing behavior of various polymer networks, we simulate the process that is utilized in experimental evaluation of self-healing [24], which involves introducing a cut in a polymer sample and allowing the sample to heal before reevaluating its mechanical properties. For this purpose, within the MD simulation box a wall of non-interacting particles is introduced in the center of the system to separate two halves of the simulation box while the system is reaching its equilibrium condition on each side, as can be seen in Fig. 2. Once this wall is removed during each system's relaxation phase, it will represent the "cut" within the polymer material. In order to re-equilibrate the self-healing system, after the wall between the two domains is removed, the two halves of the simulation box are allowed to mix and form new crosslinking bonds, i.e. the sample will self-heal. Here we use a procedure similar to the original scheme of defining bonds between crosslinking ends and backbone bonding sites. Following this step, the system

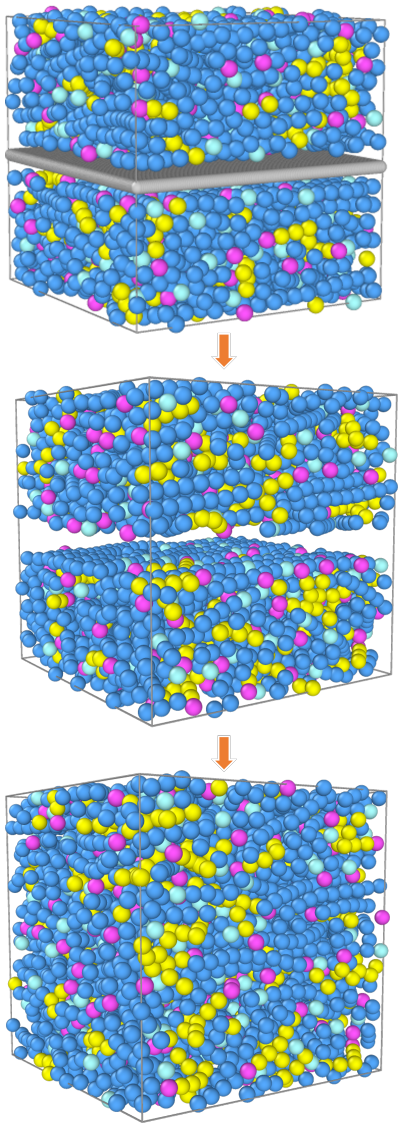

FIG. 2. MD framework for investigating self-healing properties of polymer networks. The middle wall shown in grey color introduces a "cut" into the material. After removing the middle wall, the system is allowed to self-heal by forming new bonds in the middle section.

undergoes an additional NPT relaxation process before the mechanical properties are calculated.

It is worth mentioning that the approaches described above have direct connection to experimentally relevant systems. Multiplicity of crosslinking sites can be achieved by changing the number of reactive sites on a crosslinking molecule, for instance using difunctional through thiols such as difunctional 2,2'-(Ethylenedioxy)diethanethiol, tetrafunctional Pentaerythritol tetrakis(3-mercaptopropionate) and hexafunctional thiols that can be synthesized in the laboratory [42]. The use of thiols does not limit to thiol based crosslinking, since the thiols can be reacted with alkenes containing appropriate functional groups through thiol-ene chemistry [43]. If even higher or more complex linkers were desired, a star like polymer could be synthesized to act as a multiarm crosslinker, through an arm-first type approach [44], where the initiating site contains functional groups capable of crosslinking with the linear chains. This would also approach some of the larger sized crosslinkers discussed throughout the manuscript. It is important to note that the approaches listed here do not constitute an exhaustive list of synthetic pathways, but rather indicate the feasibility of the model systems outlined in this computational study. We would like to also mention that the CG model presented in this work aims to provide a computationally simplified description of crosslinked polymer networks, in order to identify how the architecture of multi-arm crosslinked networks may affect the structure and properties of the polymer material. The trends observed based on our predictions can motivate experimental synthesis and characterization of multi-arm crosslinked systems for the first time. We note that future work will be needed to produce more accurate descriptions, such as computationally more expensive atomistic models, that include detailed descriptions of atomic bonds, dihedral angles, and improper interactions, which may provide better predictions matching experimental data obtained in the future.

III. RESULTS AND DISCUSSION

Our main goal is to elucidate the relationship between the architecture and the mechanical behavior of multi-arm crosslinked polymer networks. We first perform MD simulations to calculate the mechanical properties of multi-arm crosslinked polymers. We begin by considering the multi-arm polymer network shown in Fig. 1 (c). The crosslinkers in this system consist of three arms. As described in the previous section, the beads in each crosslinker are connected through harmonic bonds, and the angular configuration of the crosslinker is set by defining the angles between the different arms. The angle interactions are defined for two angle types as shown in Fig. 3 (a). The angle θ^b refers to the 180° angle between three consecutive beads in a backbone polymer chain and θ^{cl} refers to the angle between the arms in a multi-arm crosslinker, which in the case of the three-arm units will be 120° at equilibrium. K_θ^b and K_θ^{cl} refer to the angular stiffness for these two angle types within the MD simulations. We set a base value of $K_\theta^b = 10\epsilon$ in the LJ units for the polymer backbone chains within the MD simulations. We initially assume $K_\theta^{cl}/K_\theta^b = 1$, and utilize MD simulation to study the mechanical behavior of the system. We employ the NPT ensemble within LAMMPS to relax the system under zero pressure in order to obtain an equilibrium representation of the system. To investigate mechanical properties of the material, uniaxial strain was applied to the system in the x direction while the stresses in the y and z directions were set to zero. For consistency, we applied a fixed strain rate value of $0.05\sqrt{\frac{\epsilon}{m\sigma^2}}$ in all

of the stress-strain simulations investigating various systems of interest. Following this simulation, stress-strain curves will be obtained. Figure 3 (b) shows the resulting stress-strain curve for a three-arm crosslinked system. The stress values are normalized with respect to the maximum value of the tensile stress, i.e. the ultimate tensile stress (UTS) for this system. We also investigate the effect of the angular stiffness of the crosslinker on the mechanical performance of the 3-arm crosslinked network. We utilize K_θ^{cl}/K_θ^b, i.e. the ratio of the angular stiffness of the multi-arm crosslinker to that of the backbone polymer chain, as a control parameter that represents the angular stiffness of the 3-arm crosslinkers. We performed a series of MD simulations for various values of K_θ^{cl}/K_θ^b and calculated UTS for each case. Figure 3 (c) shows variations of UTS as a function of angular stiffness for the 3-arm crosslinked system. The results were obtained through MD simulations for various angular stiffness values of multi-arm crosslinkers ranging from 10% up to 150% of the backbone polymer angular stiffness. The UTS value for the polymer network varies by as much as 30% for various values of angular stiffness of the multi-arm crosslinker. We observe the peak UTS value around an angular stiffness ratio of 0.25, while the UTS stays fairly constant for angular stiffness ratio values in the range of $1.0-1.5$. Considering the physical nature of the system, increasing the angular stiffness of the multi-arm crosslinkers helps strengthen the polymer network mechanically, however, if the crosslinkers are too stiff, the overall network will become less mechanically strong as the crosslinkers will not be flexible enough to form bonds with various polymer backbone chains in different orientations, which in turn damages the mechanical strength of the network. Our result from MD simulations supports this logic and provides a quantitative prediction of this phenomenon, therefore, demonstrating that angular stiffness of multi-arm crosslinkers is a network feature that affects the mechanical, and potentially other, properties of crosslinked polymer networks.

Next, we investigate how increasing the number of crosslinker arms may affect the network structural architecture and the mechanical properties of the polymer material. For this purpose, we employ MD simulations of four different network compositions formed from crosslinkers with three, four, five, or six arms combined with similar background polymer chains of length $n = 100$ with 7% of the beads comprising the crosslinking sites, as mentioned in Section II. The four different systems studied here are depicted in Fig. 4 (a). We then follow the steps discussed above to calculate the uniaxial stress-strain curve for each system. Figure 4 (b) shows the resulting calculated UTS values corresponding to these four different system types.

We observe that as the number of crosslinker arms increases, the UTS and the mechanical strength of the polymer network is increased when comparing the 4-arm and 5-arm systems to the base 3-arm crosslinked systems. However, this trend does not continue as the

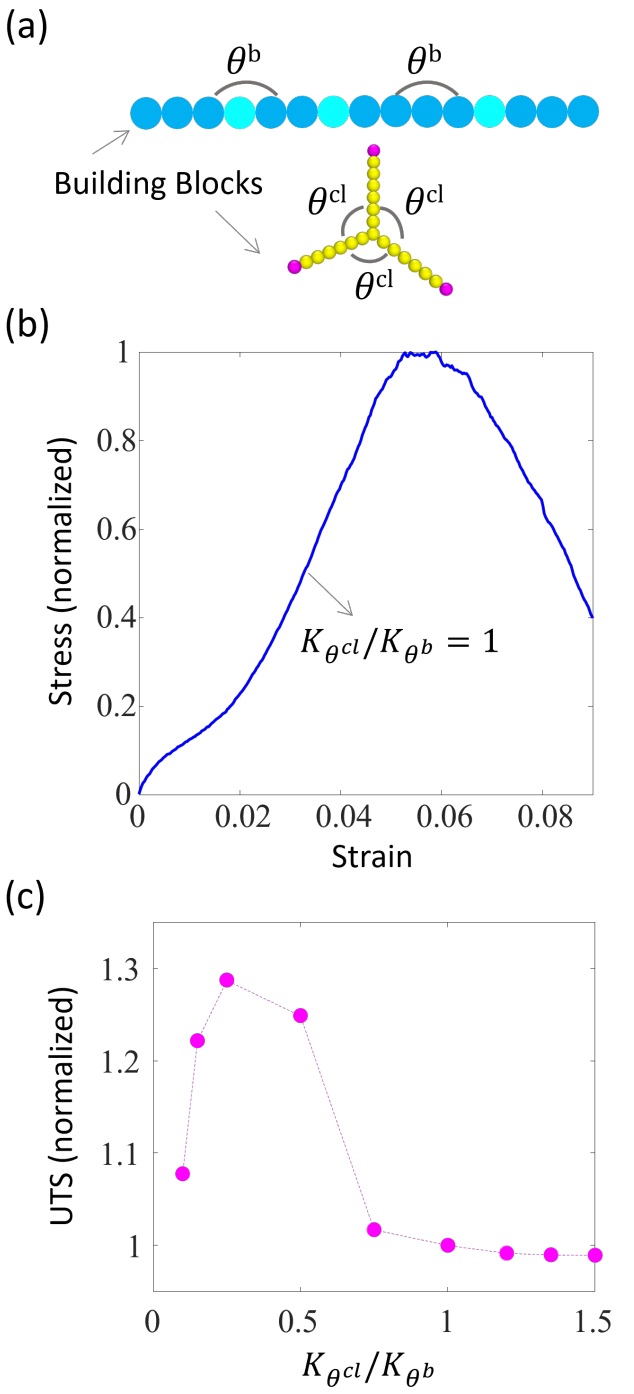

FIG. 3. (a) Schematic demonstration of various angles present in the building blocks of a multi-arm polymer network. (b) Stress-strain curve obtained from MD simulations for a polymer network composed of 3-arm crosslinkers. The stress axis is normalized with respect to the UTS. (c) Ultimate tensile stress (UTS) as a function of crosslinker angular stiffness.

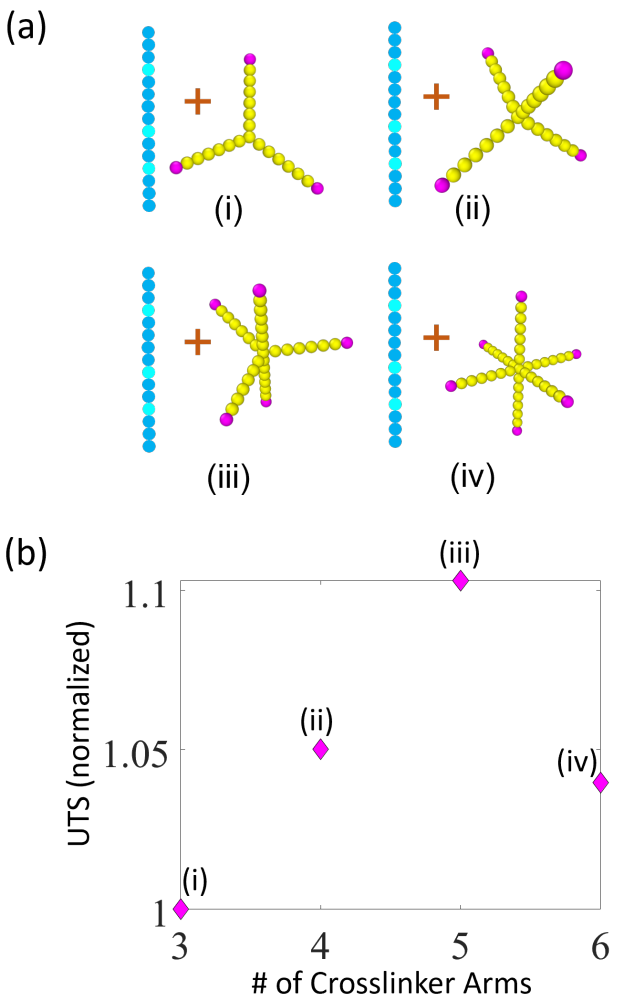

FIG. 4. (a) Schematics of the building block combinations for four different polymer network configurations obtained from crosslinking agents with different number of arms. (b) Ultimate tensile stress (UTS) reported for each of these systems. UTS values are normalized with respect to the UTS value for the 3-arm system, (i).

UTS decreases for the 6-arm crosslinked network. We note that the ratio of the available crosslinking ends of the crosslinkers to the potential crosslinking sites on the backbone chains increases proportional to the number of crosslinking arms, as the total number of crosslinkers and the number of crosslinking sites on the backbone chains were kept constant for the different systems studied. Therefore, at first glance, it appears that as the number of existing crosslinking arms increases, more connections between the crosslinkers and the backbone polymer should be established, which in turn, should increase the mechanical strength of the material. However, this is a simplistic view of the polymer network as crosslinker-backbone connection is not the only important feature of the polymer network structure. In fact, the overall network architecture includes the intertwined backbone polymers, which can interact with each other in complex ways as a result of the presence of crosslinking agents: as the number of crosslinking arms increase, more connections between the backbone chains and crosslinkers are introduced while at the same time the formation of noncovalent bonds between the backbone polymer chains may be reduced. This effect can be interpreted as a steric or excluded volume effect limiting the number of connections between the backbone chains. The combination of the factors mentioned here will eventually determine the overall mechanical behavior of the crosslinked polymer network.

In order to investigate this effect in detail, we build a graph network representation to study the architecture and the topology of the multi-arm crosslinked polymer networks in connection with their mechanical properties. Figure 5 (a) shows a sketch of the graph network model for a sample combination of backbone chains and crosslinkers. We consider all the particles of each backbone chain to form one node, as shown by blue nodes. Similarly, all the particles within each crosslinker form one node, as shown by yellow nodes. Consequently, the graph network for each system shown in Fig. 4 (a) consist of 200 blue nodes and 400 yellow nodes, for a total of 600 nodes, according to the system descriptions specified in Section II. The connections between various backbone chains and crosslinkers are represented as weighted graph edges, i.e. $w_{(i,j)}$ represents the weight of the edge connecting nodes (vertices) v_i and v_j. In order to determine the edges of the graph network corresponding to each of the systems described in Fig. 4 (a), we consider the equilibrium structure of each system which was used to calculate its mechanical properties. We then consider the existing covalent and noncovalent bonds between various building blocks to define the edges of the graph and the corresponding edge weights. For each covalent bond between a crosslinker and a backbone chain, one edge will be added between the corresponding nodes of the graph. Additionally, for each noncovalent connection present between various backbone polymer chains, one edge between the two corresponding nodes will be added to the graph. These noncovalent connections are considered between particle pairs that are closer than a cutoff distance of 1.2 times the average diameter of the two particles. Since the covalent bonds and noncovalent bonds correspond to the bonded and nonbonded interactions in the MD simulations, we chose the edge weights according to the strength of bonded and nonbonded interactions, as discussed in the Methods section. Therefore, we assign an edge weight of 1.0 for each noncovalent connection and an edge weight of 25.0 for each covalent connection within the polymer network structure. A sample overall graph structure for the 3-arm crosslinked polymer network is shown in Fig. 5 (b). Once this graph is established for each structure, quantitative characteristics of the graph can serve as descriptors for architectural features of the polymer networks.

In order to find a measure of the bonding between the

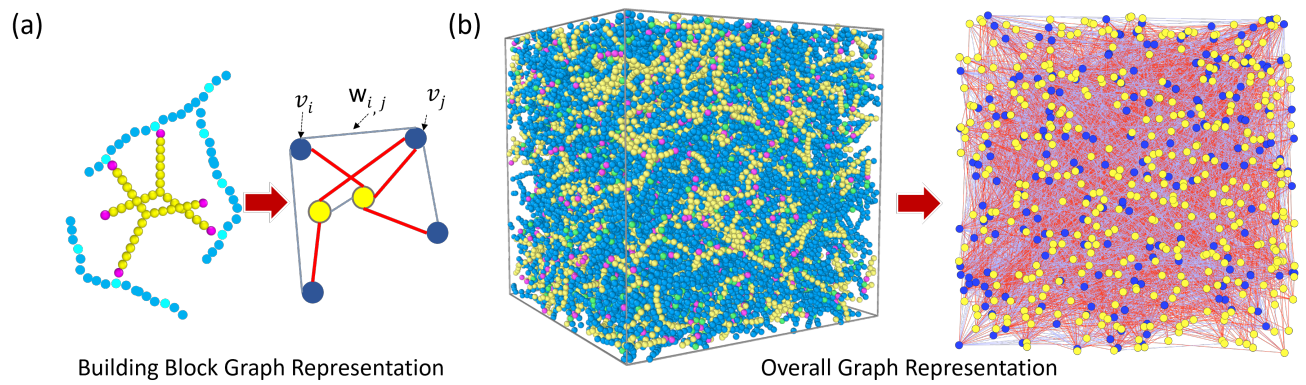

FIG. 5. (a) Graph network representation of multi-arm crosslinked polymer materials. Each backbone chain and each crosslinker are denoted as a separate node, shown by the blue and yellow nodes, respectively. Each edge is assigned a weight based on the interaction strength for the connection between the two corresponding nodes. (b) Overall structure and the corresponding graph network representation for the 3-arm crosslinked system, composed of 200 blue nodes and 400 yellow nodes. The graph sketch was prepared using the Gephi software [45].

TABLE I. Graph network characteristics for various multi-arm crosslinked polymer configurations.

System Type	**Crosslinking Connections (%)**	**Ave. Graph Node Degree**	**Graph Connectivity (λ_2)**
3-arm	37.6	0.0168	0.266
4-arm	40.6	0.0180	0.278
5-arm	57.6	0.0222	0.295
6-arm	60.3	0.0220	0.279

backbone polymer chains within the overall network, we calculate an average value of the weighted degree of the graph nodes that represent the backbone polymer chains, i.e. $\sum_{i\in V_b}\sum_{i--j\in E} w_{(i,j)}/n_b$ where $w_{(i,j)}$ denotes the edge weight between node i and its neighbor node j, V_b is the set of all nodes corresponding to the backbone chains, n_b is the size of V_b, and E is the set of all edges of the graph. This value is then normalized with respect to a reference value obtained by calculating the same equation for a (theoretical) fully-connected network with the same number of blue and yellow nodes. In addition to the connections between the backbone chains, we also quantify the overall connectivity of the graph using spectral graph theory [46]. For this purpose, we consider the smallest nonzero eigenvalue of the graph Laplacian (λ_2), known as the Fiedler number or Algebraic Connectivity, which represents a measure of the graph connectivity [46–48]. In order to obtain this value, we first calculate the normalized graph Laplacian, $\mathcal{L} = \mathcal{I} - \mathcal{D}^{-\frac{1}{2}}\mathcal{W}\mathcal{D}^{-\frac{1}{2}}$, where $\mathcal{I}$ is the identity matrix, $\mathcal{W}$ is the weighted adjacency matrix of the graph formed by the edge weight ($w_{(i,j)}$) values , and $\mathcal{D}$ is the diagonal degree matrix associated with $\mathcal{W}$. Following the calculation of the Laplacian, we find the eigenvalues of $\mathcal{L}$ to obtain the λ_2 value for each graph. All calculations are performed using the NetworkX software package [49].

Table I shows the summary of various architectural features calculated for the systems mentioned in Fig. 4 (a) based on the established graph network representations. First, we consider the crosslinking connection percentage for the 3-arm, 4-arm, 5-arm, and 6-arm systems studied, which is calculated based on the number of covalent connections between the blue and yellow nodes of the graph divided by the maximum number of crosslinking sites available on the polymer chain. This crosslinking percentage shows a consistent increase as the number of arms per crosslinker increases. Comparing this trend to the UTS values shown in Fig. 4 (b), we note that even though crosslinking percentage is an important and simple indicator of the strength of the polymer network, it does not provide a complete picture about structure-property relationships of multi-arm crosslinked networks. As mentioned earlier, the connections between various background polymer chains, which also is a direct function of the crosslinks within the network, can provide a deeper analysis of how the architecture of the polymer material is related to the resulting mechanical properties. The average node degree values reported in Table I suggest that as the number of crosslinking arms increases, the degree of connectivity between various backbone chains increases initially when comparing 3-, 4-, and 5-arm systems, and then decreases for the 6-arm system. This result points to two competing factors that affect the architecture of the polymer network and the resulting mechanical properties of the material: as the number of crosslinking arms increases more potential binding between the crosslinkers and backbone chains are possible, which should increase the mechanical strength of the material; however, at the same time increasing the number of crosslinking arms can spatially confine the backbone polymer chains and prevent the formation of noncovalent bonds between the backbone chains, thus reducing the overall strength of the polymer network. This factor

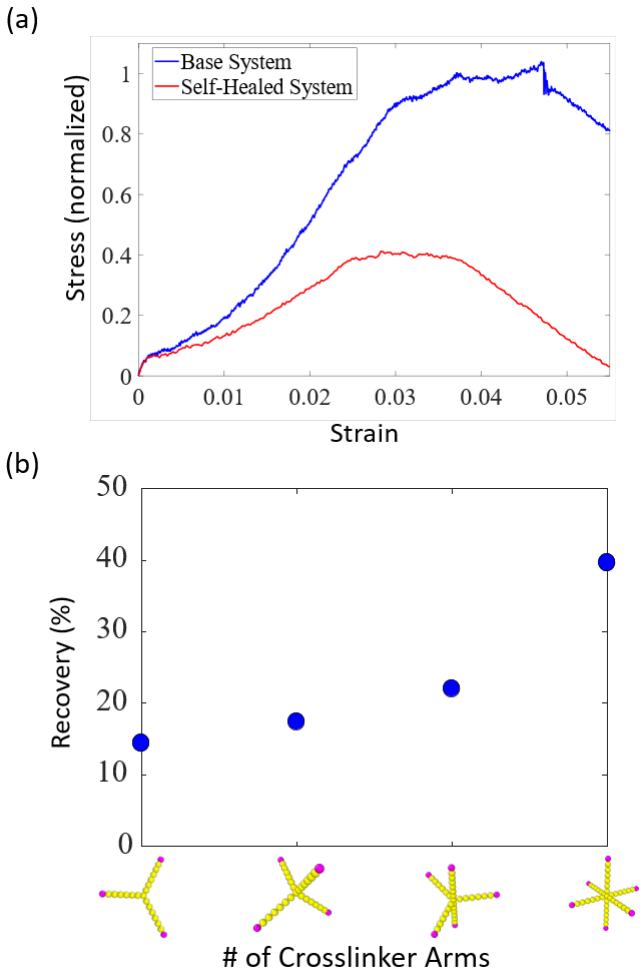

FIG. 6. (a) Comparison of the mechanical properties of the base (uncut) polymer network versus a self-healed sample. UTS values are normalized with respect to the UTS value of the base system. (b) Self-healing recovery percentage for multi-arm polymer networks with 3-, 4-, 5-, and 6-arm crosslinkers.

is further evident from the algebraic connectivity (λ_2) values calculated based on the overall graph structure of each network and the corresponding weighted edges representing covalent and noncovalent bonds present in the network. The λ_2 values in Table I show the same trend as the UTS values in Fig. 4.

Next, we study the self-healing behavior of the multi-arm crosslinked networks. For this purpose, we follow the procedure described in Section II by introducing a "cut" into each polymer system structure and calculating the resulting mechanical properties after allowing the system to heal. We then compare the mechanical performance of the self-healed sample to that of the original uncut system. As an example, Figure 6 (a) shows the stress-strain curve for the 6-armed system discussed above, for both the original and the self-healed sample. We observe that the UTS value of the curve for the self-healed system

TABLE II. Graph network characteristics for various multi-arm crosslinked polymer configurations with spherical, tetrahedral, and cubic core shapes.

System type	**Crosslinking Connections (%)**	**Ave. Graph Node Degree**	**Graph Connectivity (λ_2)**
Cubic	0.38	0.0898	0.084
Tetrahedral	0.36	0.0877	0.076
Spherical	0.31	0.0828	0.071

is around 40% of the value for the base, uncut system, which results in a 40 % recovery factor, as shown in Fig. 6 (b). The recovery factor is defined as the ratio of the UTS value of the self-healed sample to that of the original sample composed of the same building block type and architecture. We observe that as the number of arms per crosslinker increases, the self-healing recovery percentage of the crosslinked polymer material increases. This observation is aligned with the fact that once a cut is introduced in a sample, as the self-healing process starts and the backbone and crosslinker particles from the two sides start to diffuse in the middle region, a larger number of bonds are formed between the two sides of the material if more crosslinking agents are available, and the self-healed material is thus expected to be stronger. Furthermore, in the case of the 6-arm crosslinked systems, as we discussed above, the UTS value for the base system showed a decrease compared the 5-arm system. Accordingly, the self-healing recovery factor shows an even larger increase from 5-arm to 6-arm system compared to the trend observed between 3-arm, 4-arm, and 5-arm systems. This observation provides an interesting insight for the base mechanical strength of multi-arm crosslinked networks versus their self-healing behavior: utilizing larger number of arms in crosslinking agents can improve the self-healing behavior of the material at high rates, however, this improvement in self-healing behavior may happen at the cost of a reduction in the overall mechanical strength of the original polymer network.

In addition to the behavior of multi-arm systems discussed above, we also consider another category of multi-arm crosslinked polymer networks formed by various crosslinking cores of specific shapes between polymer chains, as introduced in Fig. 1. We study three distinct core shapes with cubic, tetrahedral, and spherical shapes, as shown in Fig. 7 (a). We prepared the initial configurations for each case based on the procedure described in Section II, and then calculated the corresponding mechanical properties of the equilibrium structures through finding uniaxial stress-strain curves. Each crosslinking agent core, i.e. a cubic, tetrahedral, or spherical core, is made from a set of closed packed particles, shown in the yellow color, that are covalently bonded and held together to preserve the shape of the core. The crosslinking tails are then populated on the surface of the cores being bonded to four yellow surface particles. Figure 7 (b) shows the surface density of the crosslink-

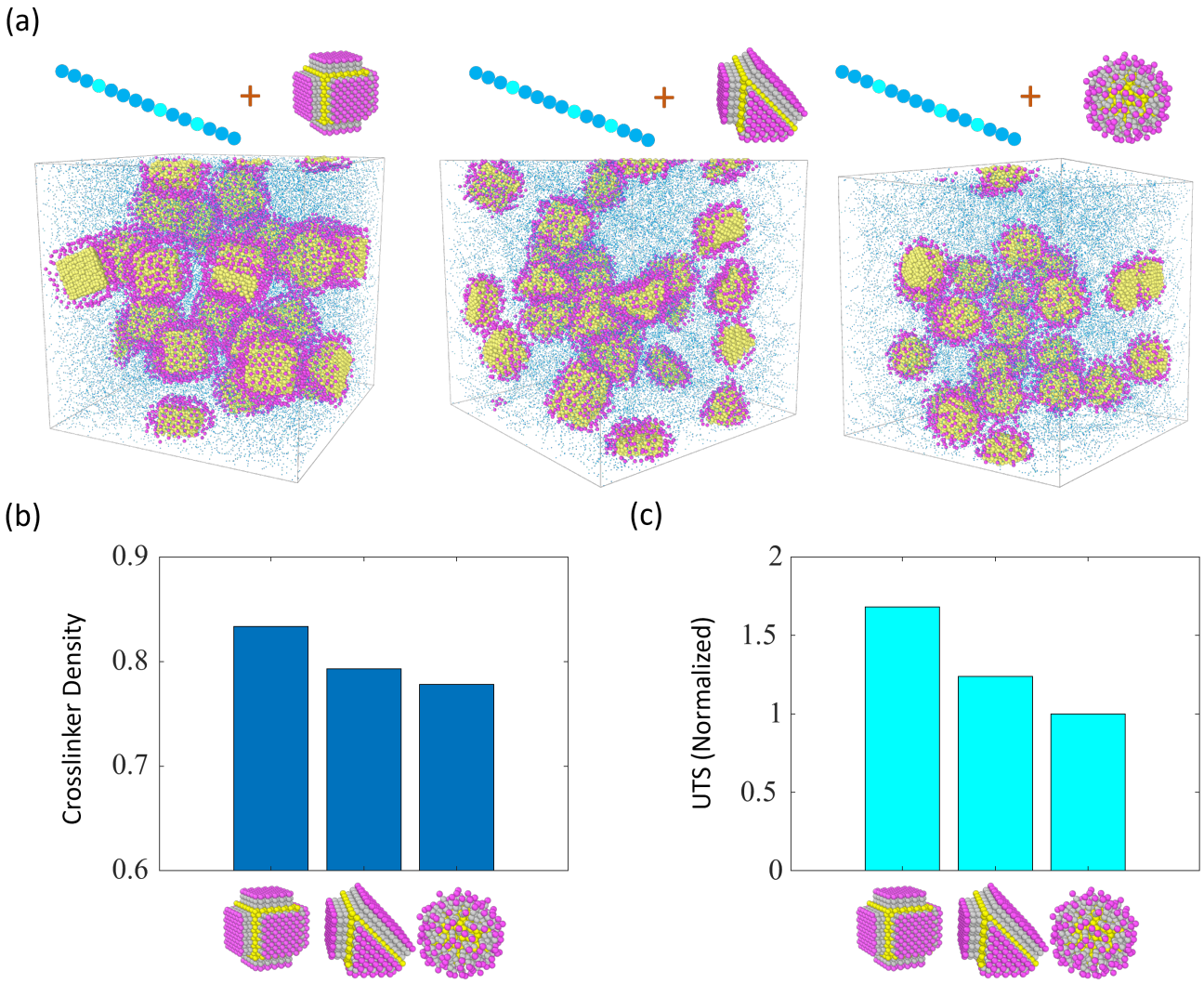

FIG. 7. (a) MD snapshot of equilibrium structures of polymer networks with cubic, tetrahedral, and spherical core shapes for the multi-arm crosslinking agents. The backbone polymer beads and the middle part of the crosslinkers are reduced in size for clarity. (b) Surface coverage density of crosslinkers calculated for a single core of each shape. (c) UTS values for the three different systems, normalized with respect to the UTS value of the spherical system.

ing tails for different core shapes, calculated based on the number of crosslinkers per unit surface area of the core. We observe that the crosslinking density for the cubic, tetrahedral, and spherical shapes are 0.84, 0.79, and 0.77, respectively. Correspondingly, the results obtained from MD simulations in Fig. 7 (c) show a similar trend, as the UTS values for the cubic and tetrahedral multi-arm systems are 1.68 and 1.24 times larger compared to the spherical system. Furthermore, in Table II the results from graph network analysis of these multi-arm polymer networks are provided. We adopt a similar approach to analyze the graph networks compared to the cases with the previous systems discussed above. We consider each backbone polymer chain and each crosslinker core as one node in the corresponding graph representation and define weighted edges based on the existing connections in the equilibrium configurations used to calculate the mechanical properties. In this case, each of the three different systems includes 720 nodes corresponding to the backbone chains and 24 nodes corresponding to the crosslinking agents. The resulting crosslinking connection percentage as well as the average graph node degree and graph connectivity all show a similar trend compared to the UTS values for systems with different crosslinking core shapes. The trends observed in these systems suggest that when the crosslinking agents are built from various core shapes, the mechanical properties of the network are mainly dominated by the crosslinking percentage and the crosslinking density which originates from the shape of the crosslinker core. Since the cores themselves are strongly-bonded elements that can reinforce the polymer network, the crosslinking percentage already provides a direct measure of the overall connectivity and the mechanical strength of the polymer net-

work as it determines the number of connections between the backbone chains and the mechanically-strong cores. This explains the reason why for the system with cubic crosslinking cores, which provides the largest crosslinking density and percentage, the UTS value is larger than the other two systems. In the case of the 3-, 4-, 5-, and 6-arm crosslinked systems studied earlier, the strongly-bonded crosslinking core does not exist, thus the combination of covalent and non-covalent bonds and the way the backbone polymer chains are interconnected becomes more significant in those systems.

IV. CONCLUSIONS

In this work, we presented a systematic study of multi-arm crosslinked polymer networks by introducing various network architecture designs and predicting the mechanical and self-healing behavior of different configurations. The computational models established in this work demonstrate that the angular stiffness of multi-arm crosslinkers can be adjusted to control mechanical strength, or equivalently, the Ultimate Tensile Stress (UTS) value of the material. We also established a graph representation of different crosslinked polymer networks to explain the intricate connection between the architecture of the network and its mechanical properties. The proposed materials and scope of investigation from an experimental standpoint was also considered.

The results of this analysis revealed that multi-arm crosslinkers introduce specific structural complexities where the combination of the connections between crosslinkers and the backbone polymers as well as the noncovalent bonding between the backbone polymers determines the overall mechanics of the system. We found that graph network properties such as algebraic graph connectivity provide suitable descriptors of the architecture of the polymer material and can help explain the emerging structure-property relationships effectively. Additionally, the study of the self-healing behavior of multi-arm crosslinked networks indicated that increasing the number of crosslinking arms improves the self-healing recovery of the polymer network, however, it can adversely affect the overall mechanical strength of the material. It is important to note, however, that the self-recovery time period was held constant for all samples investigated in this study. As shown by Watuthanthrige et. al., increasing the self-recovery duration within MD simulations will intuitively result in a larger recovery factor [24]. The computational predictions in this work can help guide future experimental work to design and establish novel multi-arm crosslinked polymer materials. Furthermore, the high dimensional parameter space associated with multi-arm crosslinked networks provides ample opportunities for generating large data sets from experiments or simulations which can pave the way for Machine Learning(ML)-based studies for design and discovery of advanced polymer materials with on-demand properties. Finally, we note that, following this study, investigation of the kinetics of multi-arm crosslinked polymer networks is an important topic of interest that needs to be addressed in future. Langevin dynamics simulations, which are computationally more expensive than MD simulations used in this work, can provide useful insight into the mechanochemical kinetics of crosslinked polymer materials [50]. In the case of multi-arm crosslinkers, this topic will be even more complex compared to simple crosslinked systems, given the fact that each crosslinker may be connected to multiple backbone chains. Therefore, additional kinetic limitations that influence the behavior of the material may be present in multi-arm systems. Future work in this area will be needed to combine experimental and theoretical methods to investigate the kinetic behavior of multi-arm crosslinked polymers, with regards to both the synthesis and mechanical characterization of such materials.

ACKNOWLEDGMENTS

This work was supported by the American Chemical Society-PRF (Award #61290) and National Science Foundation (Grant No. DMR-1749730). The authors would like to acknowledge support from Miami University's High Performance Computing group and the Ohio Supercomputer Center (Grant No. PMIU0139).

[1] H. Ma, A.-Y. Jen, and L. R. Dalton, Polymer-based optical waveguides: materials, processing, and devices, Advanced materials **14**, 1339 (2002).

[2] A. L. A, M. Behl, B. H. B, and C. Wischke, Shape-memory polymers as a technology platform for biomedical applications, Expert Rev Med Devices **7**, 357 (2010).

[3] W. F. Daniel, G. Xie, M. Vatankhah Varnoosfaderani, J. Burdynska, Q. Li, D. Nykypanchuk, O. Gang, K. Matyjaszewski, and S. S. Sheiko, Bottlebrush-guided polymer crystallization resulting in supersoft and reversibly moldable physical networks, Macromolecules **50**, 2103 (2017).

[4] H. Liang, S. S. Sheiko, and A. V. Dobrynin, Supersoft and hyperelastic polymer networks with brushlike strands, Macromolecules **51**, 638 (2018).

[5] R. J. Wojtecki, M. A. Meador, and S. J. Rowan, Using the dynamic bond to access macroscopically responsive structurally dynamic polymers, Nature materials **10**, 14 (2011).

[6] N. Roy, B. Bruchmann, and J.-M. Lehn, Dynamers: dynamic polymers as self-healing materials, Chemical Society Reviews **44**, 3786 (2015).

[7] L. Voorhaar and R. Hoogenboom, Supramolecular polymer networks: hydrogels and bulk materials, Chemical

Society Reviews **45**, 4013 (2016).
[8] N. Roy, E. Buhler, and J.-M. Lehn, Generation of supramolecular microcapsules by oxidative covalent polymerization of a ditopic supramolecular building block, Polymer Chemistry **4**, 2949 (2013).
[9] S. Monemian and L. T. Korley, Exploring the role of supramolecular associations in mechanical toughening of interpenetrating polymer networks, Macromolecules **48**, 7146 (2015).
[10] F. Herbst, D. Döhler, P. Michael, and W. H. Binder, Self-healing polymers via supramolecular forces, Macromolecular rapid communications **34**, 203 (2013).
[11] M. Nakahata, Y. Takashima, H. Yamaguchi, and A. Harada, Redox-responsive self-healing materials formed from host-guest polymers, Nature communications **2**, 511 (2011).
[12] M. Guo, L. M. Pitet, H. M. Wyss, M. Vos, P. Y. Dankers, and E. Meijer, Tough stimuli-responsive supramolecular hydrogels with hydrogen-bonding network junctions, Journal of the American Chemical Society **136**, 6969 (2014).
[13] X. Chen, M. A. Dam, K. Ono, A. Mal, H. Shen, S. R. Nutt, K. Sheran, and F. Wudl, A thermally remendable cross-linked polymeric material, Science **295**, 1698 (2002).
[14] M. Capelot, D. Montarnal, F. Tournilhac, and L. Leibler, Metal-catalyzed transesterification for healing and assembling of thermosets, Journal of the American Chemical Society **134**, 7664 (2012).
[15] C. C. Deng, W. L. Brooks, K. A. Abboud, and B. S. Sumerlin, Boronic acid-based hydrogels undergo self-healing at neutral and acidic ph, ACS Macro Letters **4**, 220 (2015).
[16] X. Yu, X. Chen, Q. Chai, and N. Ayres, Synthesis of polymer organogelators using hydrogen bonding as physical cross-links, Colloid and Polymer Science **294**, 59 (2016).
[17] E. M. Foster, E. E. Lensmeyer, B. Zhang, P. Chakma, J. A. Flum, J. J. Via, J. L. Sparks, and D. Konkolewicz, Effect of polymer network architecture, enhancing soft materials using orthogonal dynamic bonds in an interpenetrating network, ACS Macro Letters **6**, 495 (2017).
[18] B. Zhang, Z. A. Digby, J. A. Flum, E. M. Foster, J. L. Sparks, and D. Konkolewicz, Self-healing, malleable and creep limiting materials using both supramolecular and reversible covalent linkages, Polymer Chemistry **6**, 7368 (2015).
[19] N. Roy, E. Buhler, and J.-M. Lehn, Double dynamic self-healing polymers: supramolecular and covalent dynamic polymers based on the bis-iminocarbohydrazide motif, Polymer International **63**, 1400 (2014).
[20] J. A. Neal, D. Mozhdehi, and Z. Guan, Enhancing mechanical performance of a covalent self-healing material by sacrificial noncovalent bonds, Journal of the American Chemical Society **137**, 4846 (2015).
[21] D. Sophiea, D. Klempner, V. Sendijarevic, B. Suthar, and K. Frisch, Interpenetrating polymer networks as energy-absorbing materials, Interpenetrating polymer networks , 39 (1991).
[22] M. B. Zanjani, B. Zhang, B. Ahammed, J. P. Chamberlin, P. Chakma, D. Konkolewicz, and Z. Ye, Computational investigation of the effect of network architecture on mechanical properties of dynamically cross-linked polymer materials, Macromolecular Theory and Simulations **28**, 1900008 (2019).
[23] N. De Alwis Watuthanthrige, D. Dunn, M. Dolan, J. L. Sparks, Z. Ye, M. B. Zanjani, and D. Konkolewicz, Tuning dual-dynamic network materials through polymer architectural features, ACS Applied Polymer Materials **4**, 1475 (2022).
[24] N. D. A. Watuthanthrige, B. Ahammed, M. T. Dolan, Q. Fang, J. Wu, J. L. Sparks, M. B. Zanjani, D. Konkolewicz, and Z. Ye, Accelerating dynamic exchange and self-healing using mechanical forces in crosslinked polymers, Materials Horizons **7**, 1581 (2020).
[25] O.-K. Park, W. Lee, J. Y. Hwang, N.-H. You, Y. Jeong, S. M. Kim, and B.-C. Ku, Mechanical and electrical properties of thermochemically cross-linked polymer carbon nanotube fibers, Composites Part A: Applied Science and Manufacturing **91**, 222 (2016).
[26] M. Ozmaian, D. Jasnow, A. Eskandari Nasrabad, A. Zilman, and R. D. Coalson, Effects of cross-linking on partitioning of nanoparticles into a polymer brush: Coarse-grained simulations test simple approximate theories, The Journal of Chemical Physics **148**, 024902 (2018).
[27] F. Syed, S. Zainuddin, A. Willis, M. Hosur, and S. Jeelani, Crosslinking and interfacial behavior of carboxylic functionalized carbon nanotube epon nanocomposites: A molecular dynamic simulation approach, SN Applied Sciences **1**, 1 (2019).
[28] E. B. Stopler, O. J. Dodo, A. C. Hull, K. A. Weaver, P. Chakma, R. Edelmann, L. Ranly, M. B. Zanjani, Z. Ye, and D. Konkolewicz, Carbon nanotube enhanced dynamic polymeric materials through macromolecular engineering, Materials Advances **1**, 1071 (2020).
[29] B. Arab and A. Shokuhfar, Molecular dynamics simulation of cross-linked urea-formaldehyde polymers for self-healing nanocomposites: prediction of mechanical properties and glass transition temperature, Journal of molecular modeling **19**, 5053 (2013).
[30] H. Ma and Z. Tian, Effects of polymer chain confinement on thermal conductivity of ultrathin amorphous polystyrene films, Applied Physics Letters **107**, 073111 (2015).
[31] D. V. Guseva, V. Y. Rudyak, P. V. Komarov, B. A. Bulgakov, A. V. Babkin, and A. V. Chertovich, Dynamic and static mechanical properties of crosslinked polymer matrices: multiscale simulations and experiments, Polymers **10**, 792 (2018).
[32] K. Yu, A. Xin, and Q. Wang, Mechanics of self-healing polymer networks crosslinked by dynamic bonds, Journal of the Mechanics and Physics of Solids **121**, 409 (2018).
[33] G. Singh and V. Sundararaghavan, Modeling self-healing behavior of vitrimers using molecular dynamics with dynamic cross-linking capability, Chemical Physics Letters **760**, 137966 (2020).
[34] Z. Luo, Z. Yang, Z. Fei, and G. Su, Investigating mechanical properties of cross-linked sio2 and polyimide through molecular dynamics simulation, Polymer Bulletin **77**, 5213 (2020).
[35] Y. Fang, T. Yue, S. Li, Z. Zhang, J. Liu, and L. Zhang, Molecular dynamics simulations of self-healing topological copolymers with a comblike structure, Macromolecules **54**, 1095 (2021).
[36] M. Salman, W. Verestek, and S. Schmauder, Atomistic-scale modeling of nano-clay-filled shape memory polymers, Computational Materials Science **188**, 110246 (2021).
[37] X. Zheng, H. Yang, Y. Sun, Y. Zhang, and Y. Guo,

A molecular dynamics simulation on self-healing behavior based on disulfide bond exchange reactions, Polymer **212**, 123111 (2021).

[38] G. S. Grest, Structure of many-arm star polymers in solvents of varying quality: A molecular dynamics study, Macromolecules **27**, 3493 (1994).

[39] E. Mahmoudinezhad, A. Marquardt, G. Eggeler, and F. Varnik, Molecular dynamics simulations of entangled polymers: The effect of small molecules on the glass transition temperature, Procedia Computer Science **108**, 265 (2017).

[40] I. Lyubimov, M. G. Wessels, and A. Jayaraman, Molecular dynamics simulation and prism theory study of assembly in solutions of amphiphilic bottlebrush block copolymers, Macromolecules **51**, 7586 (2018).

[41] S. Plimpton, P. Crozier, and A. Thompson, Lammps-large-scale atomic/molecular massively parallel simulator, Sandia National Laboratories **18**, 43 (2007).

[42] R. A. Ortiz, E. A. O. Blandón, and R. G. Santos, Synthesis of novel hexathiolated squalene and its thiol-ene photopolymerization with unsaturated monomers, Green and Sustainable Chemistry **2** (2012).

[43] C. E. Hoyle and C. N. Bowman, Thiol–ene click chemistry, Angewandte Chemie International Edition **49**, 1540 (2010).

[44] H. Gao and K. Matyjaszewski, Arm-first method as a simple and general method for synthesis of miktoarm star copolymers, Journal of the American Chemical Society **129**, 11828 (2007).

[45] M. Bastian, S. Heymann, and M. Jacomy, Gephi: An open source software for exploring and manipulating networks (2009).

[46] D. Spielman, Spectral graph theory, Combinatorial scientific computing (2012).

[47] M. Fiedler, Laplacian of graphs and algebraic connectivity, Banach Center Publications **25**, 57 (1989).

[48] M. Fiedler, Algebraic connectivity of graphs, Czechoslovak mathematical journal **23**, 298 (1973).

[49] A. A. Hagberg, D. A. Schult, and P. J. Swart, Exploring network structure, dynamics, and function using networkx, in *Proceedings of the 7th Python in Science Conference*, edited by G. Varoquaux, T. Vaught, and J. Millman (Pasadena, CA USA, 2008) pp. 11 – 15.

[50] R. Adhikari and D. E. Makarov, Mechanochemical kinetics in elastomeric polymer networks: heterogeneity of local forces results in nonexponential kinetics, The Journal of Physical Chemistry B **121**, 2359 (2017).